A Wideband Waveguide Transition Design with Modified Dielectric Transformer Using Edge-Based Tetrahedral Finite-Element Analysis

Ruey-Beei Wu

Abstract—**A waveguide transition analysis approach has been established to deal with arbitrary shaped three-dimensional (3-D) waveguide discontinuity problems, by hybridizing the edge-based tetrahedral finite-element method for the junction region and the analytic modal expansion technique for the waveguide region. Several unique features have been imbedded in the analysis, including a variational formula for the scattering coefficients, a modified Delaunay triangulation for the mesh generation, and a frontal solution technique for the sparse matrix solution. As a result, the analysis is verified to be accurate, versatile, and efficient through extensive comparisons with the theoretical and measurement data in the available literature. The approach is then applied to design a rectangular to dielectric-filled circular waveguide transition with less than −20 dB return loss over a 40% bandwidth by using a suitable modified dielectric rod transformer.**

I. Introduction

DIELECTRIC-FILLED circular waveguides have important applications in many microwave devices, e.g., isolators and phase shifters [1]. In these devices, although the main bodies are in a circular shape, the input/output ports in standard rectangular waveguides are always required. In light of the abrupt change in the waveguide shapes and the constitutive dielectrics, it has been a great challenge to deal with such waveguide transition problems. To achieve good transition, the dielectric should somewhat intrude the rectangular waveguide portion by a certain length and with a suitable shape. Without available literature on this subject, the design of such a transition is up to now been accomplished mostly by trial and error, experimentally.

In light of the vast applications, waveguide discontinuity problems have been dealt with by a lot of researchers for a long time. Traditionally, most of the investigations are based on the mode or field matching method originally proposed by Wexler [2], which is basically limited to step-like discontinuities, say [3], [4]. Recently, the numerically intensive but flexible finite difference time domain method has also been tried for waveguide junction problems [5]. However, the applications have been plagued by its difficulty in modeling the curved boundary and its inaccuracy in handling waveguide boundary conditions.

Manuscript received June 11, 1995; revised March 20, 1996. This was supported in part by the National Center for High-Performance Computing, Republic of China, under Grant NCHC-85-03-003.

The author is with the Department of Electrical Engineering, National Taiwan University, Taipei, Taiwan, Republic of China.

Publisher Item Identifier S 0018-9480(96)04702-3.

Among the available techniques, the finite-element method (FEM) is probably the best one due to its capability of analyzing three-dimensional (3-D) waveguide junctions which may be inhomogeneously loaded and of arbitrary shape. In order to confine the solution region, FEM should be hybridized with some analytic expression, such as the eigenmode expansion, to include the field in the unbounded exterior region. In the beginning, the hybrid FEM was implemented to deal with scattering of dielectric coated cylinders [6] and propagation characteristics of dielectric waveguides [7]. Later on, it was applied to model two-dimensional (2-D) planar MMIC devices [8] and more recently, 3-D general waveguide discontinuity problems [9], [10]. Together with the development of the edge elements [11] to eliminate the occurrence of spurious modes, the hybrid FEM has become a reliable method to deal with many practical 3-D problems. Based on this method, computer software has been developed and is available commercially [12].

Even so, some fundamental problems still exist in FEM. One of them is the stationary property of the formulation. Basically, FEM relies on a functional which is in a form similar to the variational principle proposed by Chen *et al.* [13]. It is not difficult to show that the functional is stationary. However, as pointed out in [11], it remains unresolved whether the formula to calculate the desired physical parameters, e.g., the scattering coefficients, is stationary. As a result, the accuracy of the calculated results may not be the optimum one obtainable in the linear function space constructed to by the basis functions.

Another problem is how to achieve a reliable mesh generation for general 3-D objects. Although seldom addressed in previous literature, the difficulty in automatic tetrahedral mesh generation and the related database management has strongly hindered the popularity of FEM. The Delaunay triangulation [14] has already been successfully employed for 2-D electromagnetic problems [15]. Although theoretically straightforward [16], the generalization to 3-D problems is not so fruitful in practical applications. Some previous trail of this algorithm reveals, but fails to prove, that the resultant mesh includes a lot of undesired "sliver" elements and is not the optimal one for 3-D FEM applications. Furthermore, the algorithm for more complicated structures usually ends as a vain attempt due to the finite digit accuracy in numerical computation [17].

This paper starts in Section II with a unified variational reaction derivation to the functional, which is then discretized

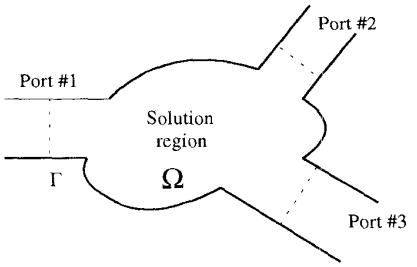

Fig. 1. A typical waveguide discontinuity problem.

to yield a matrix equation for the unknown field by the edge-based tetrahedral FEM. Not only the functional but also the calculation formula for the desired scattering parameters are shown to be stationary over the solution field. Section III describes a modified Delaunay triangulation algorithm for the automatic mesh generation. A program suitable for general 3-D waveguide junction problems has been successfully tailored in the personal computer. Accuracy of the program is validated in Section IV via comparisons with available theoretical and/or experimental results in the literature. The design of a waveguide junction with a dielectric transformer is discussed in Section V. Finally, conclusions are drawn in Section VI.

II. Variational Reaction Formulation

Fig. 1 shows a typical waveguide discontinuity problem where several waveguides are connected through a junction region which may be of arbitrary shape and may include several different materials. To facilitate the formulation, consider the simplest case of a single waveguide. With exact field distribution in the waveguide junction inaccessible, numerical methods should be resorted to in finding the approximate solution.

Being not exact, the approximate field solution $(\vec{E}, \vec{H})$ must be supported by some source distribution

$$\vec{J} = \nabla \times \vec{H} - j\omega\epsilon\vec{E},$$

$$\vec{M} = -\nabla \times \vec{E} - j\omega\mu\vec{H}. \tag{1}$$

It is required that the supporting source should be as close as possible to the exact source $(\vec{J}_0, \vec{M}_0)$, which is zero everywhere in the present scattering problem. The requirement, however, is difficult to realize since it involves two vector continuums in an unbounded region.

Fruitful constraints which reduce the requirement to a smaller region will make the numerical solution easier and more accurate. Several formulations are possible, among which the $\vec{E}$-formulation is to be employed here. We enforce $\vec{M} = \vec{0}$ everywhere, which is possible if we treat $\vec{E}$ as unknown and express $\vec{H}$ in terms of $\vec{E}$ by

$$\vec{H} = \frac{-1}{j\omega\mu}\nabla \times \vec{E}. \tag{2}$$

It is not difficult to enforce that $\vec{J} = \vec{0}$ inside the semi-infinitely long waveguide region. By the modal expansion, the tangential fields in the waveguide region $(z < 0)$ can be expressed as

$$\vec{E}_t(\vec{r}) = \sum_{n=1}^{\infty} (a_n^i e^{-\gamma_n z} + a_n^r e^{\gamma_n z})\vec{e}_{tn}(s, y),$$

$$\vec{H}_t(\vec{r}) = \sum_{n=1}^{\infty} (a_n^i e^{-\gamma_n z} - a_n^r e^{\gamma_n z})\vec{h}_{tn}(x, y) \tag{3}$$

where $(\vec{e}_{tn}, \vec{h}_{tn})$ is the tangential field distribution of the nth mode, γ_n is the complex propagation constant, a_n^i is the given modal amplitude of incident wave, and a_n^r is the unknown modal amplitude of reflected wave. Due to the modal orthogonality

$$\int \vec{e}_{tm} \times \vec{h}_{tn} \cdot \hat{z}\, d\Gamma = \delta_{mn} \tag{4}$$

the unknown reflected wave can be obtained from the electric field along the boundary $(z = 0)$ by

$$a_n^r = \int_{z=0} \vec{E} \times \vec{h}_{tn} \cdot \hat{z}\, d\Gamma - a_n^i. \tag{5}$$

The remaining requirement that $\vec{J} = \vec{0}$ in the junction region is very difficult to accomplish analytically. Instead, we employ a lot of testing functions $\vec{E}^a$ and require that for each one of them, the weighted average over the junction region Ω should be zero, ie,

$$I(\vec{E}, \vec{E}^a) \equiv \int_{\Omega} \vec{J} \cdot \vec{E}^a\, d\Omega = 0. \tag{6}$$

Note that $\vec{J}$ is expressible in terms of $\vec{E}$ as depicted by (1) and (2). Intuitively, the supporting error source $\vec{J}$ can be made arbitrarily small almost everywhere if sufficient number of testing functions are imposed.

After substituting $\vec{J}$ by (1) and taking integration by part, (6) can be expressed by

$$I(\vec{E}, \vec{E}^a) = \oint_{\Gamma} \vec{H} \times \vec{E}^a \cdot \hat{n}\, d\Gamma - \int_{\Omega} (j\omega\epsilon\vec{E} \cdot \vec{E}^a - \vec{H} \cdot \nabla \times \vec{E}^a)\, d\Omega. \tag{7}$$

The $\vec{H}$ field on the waveguide boundary can be written in terms of the boundary $\vec{E}$ field by (3) and (5). The contribution from the remaining boundary, the metallic boundary of the junction region, is zero since the tangential electric field is enforced zero there. The $\vec{H}$ field in the function region can be expressed in terms of $\vec{E}$ by (2). As a result, (7) becomes

$$I(\vec{E}, \vec{E}^a) = -\int_{\Omega} \left(j\omega\epsilon\vec{E} \cdot \vec{E}^a + \frac{1}{j\omega\mu}\nabla \times \vec{E} \cdot \nabla \times \vec{E}^a \right) d\Omega - \sum_{n=1}^{\infty} \int_{z=0} \vec{E} \times \vec{h}_{tn} \cdot \hat{z}\, d\Gamma \int_{z=0} \vec{E}^a \times \vec{h}_{tn} \cdot \hat{z}\, d\Gamma + 2\sum_{n=1}^{\infty} a_n^i \int_{z=0} \vec{E}^a \times \vec{h}_{tn} \cdot \hat{z}\, d\Gamma \tag{8}$$

which should equal zero for all the testing functions.

Noting that (8) is symmetric with respect to $\vec{E}$ and $\vec{E}^a$, we can yield a variational equation

$$\delta L = 0;$$

$$L = \frac{1}{2} I(\vec{E}, \vec{E}) + \sum_{n=1}^{\infty} a_n^i \int_{z=0} \vec{E} \times \vec{h}_{tn} \cdot \hat{z}\, d\Gamma \qquad (9)$$

which can be shown to be stationary at the exact field $\vec{E}_0$. The functional L is expressed solely in terms of the unknown electric field in the solution region. In contrast to the previous approach, say [8], [9], the present variational equation does not include any waveguide modal coefficients as the unknowns. Instead, the scattering parameters are obtained from the electric field *a posteriori* by employing (5).

It is interesting to depict the physical meaning of the functional L. The term $I(\vec{E}, \vec{E})$ is zero since (8) is zero for arbitrary $\vec{E}^a$, including the case that $\vec{E}^a = \vec{E}$. The second term in the right-hand side of (9) is directly related to the modal amplitudes of the reflected waves as evident by (5). As a result, stationary L implies stationary reflection coefficient S_{11}. This contradicts the statement made by Bossavit [11] claiming that the general variational principle proposed by Chen *et al.* [13] is useless.

The generalization of the expression (8) or (9) to junction structures consisting of more than one waveguides is straightforward. To take into account the contributions from all the waveguides, one needs only to include a summation sign over all the waveguide ports in front of the series summation of the boundary terms.

It is a typical procedure to discretize (8) for numerical computation by the edge-based tetrahedral FEM [9]. The junction region is first divided into many small tetrahedral elements. Inside each tetrahedral element, the electric fields $\vec{E}$ and $\vec{E}^a$ are expanded by the Whitney one-form edge basis [11] with the tangential field components along the six edges as the expansion coefficients. Substituting the fields into (8) and taking the volume and surface integrals, (8) can be cast into the form

$$I(\vec{E}, \vec{E}^a) = -\mathbf{e}^{\mathbf{a}T} \left[\left\{ \mathbf{G} + \sum_{n=1}^{\infty} \mathbf{b_n} \mathbf{b_n}^T \right\} \mathbf{e} - 2 \sum_{n=1}^{\infty} a_n^i \mathbf{b_n} \right] \qquad (10)$$

where $\mathbf{e^a}$ and $\mathbf{e}$ denote the column vectors constituted by all the expansion coefficients for the fields $\vec{E}^a$ and $\vec{E}$, respectively, superscript T denotes the transpose, $\mathbf{G}$ is a sparse matrix obtained by assembling the volume integrals over all the elements, and $\mathbf{b_n}$ is a column vector formed by assembling the surface integrals taken between the nth waveguide mode and all those elements with one facet on the waveguide boundary. Since (10) is zero for arbitrary $\mathbf{e^a}$, the resultant column vector inside the bracket should be zero. This yields a matrix equation for the unknown column vector $\mathbf{e}$.

III. Mesh Generation

It is well accepted that the tetrahedral elements are the most versatile to model 3-D structures of arbitrary shapes. However, how to devise a reliable and robust algorithm which can automatically generate a good mesh for almost any 3-D structures has been always a bothersome problem.

The Voronoi tessellation and the dual Delaunay triangulation have proven the existence of the best mesh for given nodal points in the 2-D plane [14]. The resultant mesh is optimum in the sense that its minimum angle is maximum among all the possible meshes connecting those nodal points. It is well known that a mesh T is a Delaunay triangulation if and only if no vertex is interior to any circumcircle of a triangle of T. This property can be generalized to 3-D space if the triangle and circumcircle are replaced by the tetrahedron and circumsphere, respectively.

Based on this property, a node insertion algorithm which is easy to understand and applicable to multidimensional space has been proposed [16]. The algorithm starts from an initial mesh consisting of a single tetrahedron which is large enough to enclose all the nodal points. New internal tetrahedra are formed as the points are entered into the mesh one at a time. At each stage of the process, a search is made for all current tetrahedra to identify those whose circumspheres contain the newly entered point, say P. The union of all such tetrahedra forms what we call an insertion polyhedron, which contains P but no other previously inserted points in its interior. All the tetrahedra in the insertion polyhedron are cleared to make room for the new created tetrahedra which are formed by connecting P to all triangular facets of the polyhedron. When combined with the tetrahedra outside the polyhedron, the resultant new mesh defines a Delaunay triangulation which contains the newly added point. The process repeats until all the points are included.

Although theoretically exact, the Delaunay triangulation usually fails due to the existence of the nearly degenerate cases in practice. Degenerate cases happen when the newly inserted point P appears to lie very close to the circumsphere surface associated with a certain existing tetrahedron. Whenever the distance of P to any existing circumsphere is less than the accumulated computer truncation error, there is the danger of making an incorrect or inconsistent decision regarding rejection or selection of the tetrahedron. This in turn produces structural inconsistencies, ie, overlapping tetrahedra or gaps in the mesh, and eventually halts the triangulation process. Fig. 2 shows a typical example where P is close to the circumcircles of the triangles ΔADB, ΔBEC, ΔDGE, and ΔEGF. Structural inconsistency happens when ΔEGF is selected while ΔDGE is rejected.

A simple remedy was proposed in [17], which suggested a slight perturbation of the coordinates of the newly entered nodal point whenever the degenerate case happens. For structures with more nodal points, it becomes more probable that the newly inserted point is close to the circumsphere surfaces of many existing tetrahedra. As a result, it is difficult to properly tune the point into a region away from all these surfaces. Furthermore, the tuned point may become close to the circumsphere surfaces of other tetrahedra. The tuning process should be tried again and again. Our practice shows that this remedy is unsuccessful, even when the double precision computation is employed.

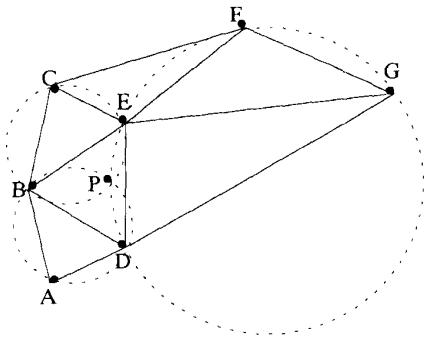

Fig. 2. Degenerate case where the new point P is close to circumcircles of existing triangles.

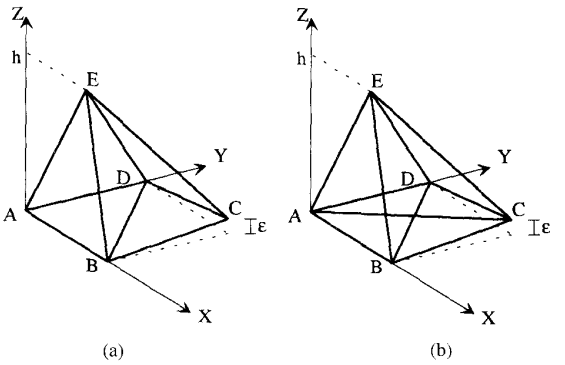

Fig. 3. Two possible mesh division for five nodal points. (a) Good mesh. (b) Bad mesh.

This analysis adopts a better strategy which enforces the structural consistency in the node insertion process. The strategy is as regards selecting suitable tetrahedra to form the insertion polyhedron for the newly inserted point P. It is described as follows.

1) Allowing a suitable threshold of computation error, all the tetrahedra whose circumspheres may possibly enclose P are activated.
2) Starting with the tetrahedron whose circumcenter is closest to P, the insertion polyhedron grows by including all those activated tetrahedra which can connect the polyhedron by at least one surface. The remaining tetrahedra are isolated from the insertion polyhedron. They are deactivated.
3) Check the volume of the tetrahedron formed by P and each triangular facet of the insertion polyhedron. If the volume is negative, this implies that some overlapping tetrahedra will result. In that case, the activated tetrahedron which contributed the triangular facet is deactivated. Repeat steps 2) and 3) for all those tetrahedra remaining activated until the volume of each new created tetrahedron is positive.

This strategy assures the structural consistency of the newly constructed mesh in each step, although the Delaunay property may be slightly sacrificed. The decision regarding the selection or rejection does not rely solely on the Delaunay property, which suffers from the computer truncation error. Rather, it sticks to the structural consistency which is combinatorial and will not deteriorate as the node insertion proceeds.

Roughly speaking, the Delaunay triangulation results in a mesh which has well proportioned lengths (areas) among the comprising sides (surfaces) of all the generated triangular (tetrahedral) elements. A triangle can be uniquely defined by its three side lengths. However, it is not sufficient to determine the tetrahedron given the areas of its four surfaces. As a result, the Delaunay triangulation in the 3-D case may create some sliver tetrahedra, in which the four facets are well proportioned but the volume is very small. This problem usually happens if there are any four nearby points which are almost, but not exactly, coplanar.

To explain this occurrence, consider a simple configuration in Fig. 3 that consists of five nodal points: $A(0, 0, 0)$, $B(2, 0, 0)$, $C(2, 2, \epsilon)$, $D(0, 2, 0)$, and $E(1, 1, h)$, where ϵ is a small positive number and $h > 0$. Note that the four points A, B, C, D are nearly coplanar. Fig. 3 shows the two possible mesh divisions for this configuration. One consists of two tetrahedra, $ABDE$ and $BCDE$, while the other has three tetrahedra, $ACDE$, $ABCE$, and $ABCD$. Obviously, the latter is worse since it includes a sliver tetrahedron $ABCD$. For the former mesh, it is easy to verify that the center and radius of the circumsphere of $ABDE$ are $(1, 1, z_0)$ and $h-z_0$, respectively, where $z_0 = \frac{h}{2} - \frac{1}{h}$. The mesh will satisfy the Delaunay property if and only if the point C is outside of the circumsphere, ie,

$$(1)^2 + (1)^2 + (z_0 - \epsilon)^2 > (h - z_0)^2. \tag{11}$$

In other words, the Delaunay triangulation yields to the bad mesh shown in Fig. 3(b) when $h > \sqrt{2}$ and $0 < \epsilon < h - \frac{2}{h}$.

The sliver tetrahedra are undesirable since (8) requires taking the curl of its edge basis and the curl may be nearly singular. Once the bad submesh shown in Fig. 3(b) is located it should be rearranged into the good submesh shown in Fig. 3(a) [17]. More general consideration is also available for complicated situations where the bad submesh involves more than three tetrahedra [16].

IV. Numerical Results and Comparisons

A general waveguide transition analysis program WG2WG has been established to deal with electromagnetic scattering off an arbitrarily shaped 3-D junction between several circular and/or rectangular waveguides. Based on the slicing approach, nodal points are chosen to discretize the solution region as well as reasonably model the shape of the conductor and/or dielectric interfaces [17]. The modified Delaunay triangulation is applied to construct the mesh, under the constraint that no tetrahedron may intersect different material regions.

Applying FEM procedure yields to a matrix equation for the field unknowns. As far as the scattering parameters are concerned, only the unknowns along the boundary are relevant. It will be especially advantageous to solve the matrix equation by the frontal solution technique [19]. All the unknowns interior to the solution region are eliminated rather than solved [7]. The final boundary matrix, being independent of

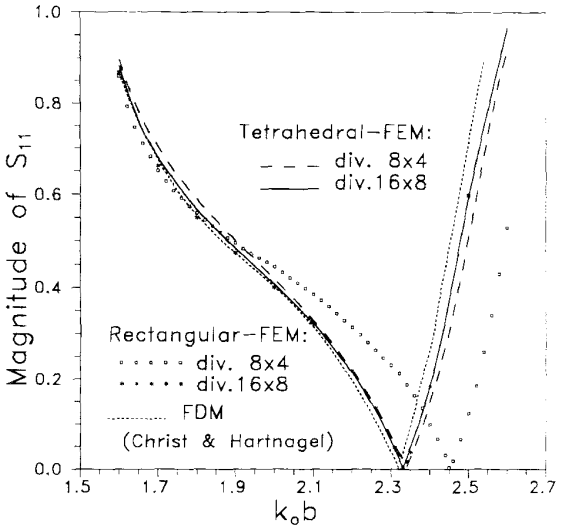

Fig. 4. Calculated reflection coefficient for a dielectric loaded rectangular waveguide. Comparisons among finite difference method, rectangular elements based FEM [10], and the present analysis.

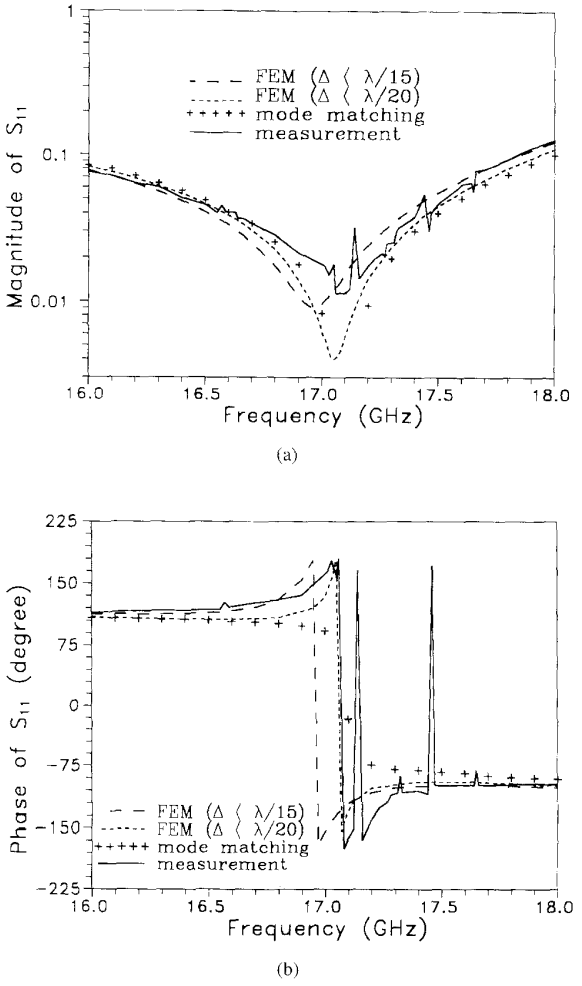

Fig. 5. Reflection coefficient for a step transformer between WR-62 and circular waveguides. (a) Magnitude. (b) Phase. Comparisons among mode matching method, measurement [4], and the present analysis.

the excitation on the waveguide ports, is LU-decomposed. By specifying the excitation in the right-hand vector, the boundary unknowns can be solved by forward and backward substitutions and the desired scattering matrix can be obtained. This approach is very efficient in memory requirement such that the program can be executed in almost any computer platform. Actually, all the following results are executed using a notebook IBM/PC-486 personal computer.

The number of waveguide modes should be truncated to perform the numerical computations. It is well known that the relative convergency problem inherent in the mode matching method may happen due to truncating a double series expansion [3]. This analysis suggests a natural way in the truncation of modes according to their cutoff frequencies, which can apply to not only rectangular but also circular or more general waveguides. In addition, it will be advantageous to intentionally choose the waveguide boundary plane slightly away from the junction region. Although this unavoidably enlarges the solution region, it can assure that even the extremely high order modes that may be excited at the junction plane exponentially decay to be negligible after propagating through this short waveguide section. As a result, several tens of modes are more than enough to account for all the higher order modes' effects, free of any relative convergency problem.

Being flexible, the WG2WG program has been applied to analyze many waveguide discontinuity problems available in the literature. The comparisons have been found to be satisfactory; two examples will be shown here. The first example considers a rectangular waveguide of size $2b \times b$ loaded with a material of size $0.888b \times 0.399b$, length $0.8b$, and dielectric constant $\epsilon_r = 6$ [10, Fig. 3]. Since the structure can be modeled as well by rectangular mesh, both the results by rectangular elements based FEM and the finite difference method (FDM) are available in the literature [10, Fig. 5]. In the present analysis, the tetrahedral elements are employed to model the structure. Two meshes with division sizes similar to those adopted in [10, Fig. 4] have been tried. The results are shown in Fig. 4 by solid and dashed curves, respectively. Although requiring more unknowns, the present FEM analysis exhibits better accuracy than its counterpart using rectangular elements in [10]. Nonetheless, both methods yield almost identical results when using the finer mesh, in this case at least 15 division cells per wavelength in each material over the frequency band of interest. This verifies the capability of the present analysis in dealing with the dielectric loaded junctions.

The second example considers a transition between a WR-62 rectangular guide and a circular guide of diameter 19.5 mm through an intermediate rectangular guide of size 15 mm $\times$ 12.4 mm and length 4.35 mm [4, Fig. 3]. The transition is designed to achieve a less than -20 dB return loss over an 11% bandwidth. Note that the structure can not be well modeled by all those methods which rely on a rectangular mesh. In addition, the reflection coefficient, being very small in a wide frequency range, can not be predicted successfully

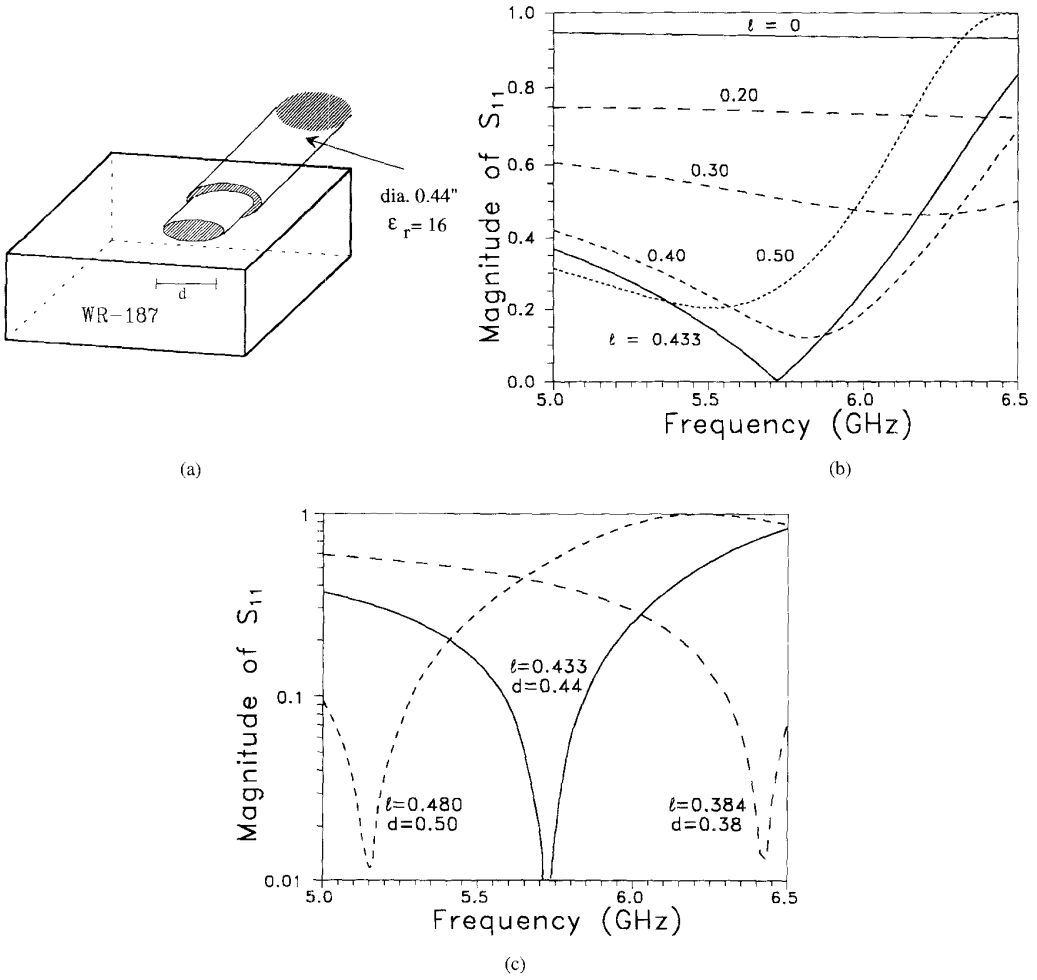

Fig. 6. Transition WR-187 to circular waveguide formed by a dielectric rod of diameter d and length l. (a) Structure. (b) Reflection coefficients with fixed $d = 0.44$ in and length l as a parameter. (c) Reflection coefficients of three matched designs.

by numerical methods without high accuracy. The magnitude and phase of the calculated results by the present FEM analysis are shown in Fig. 5(a) and (b), respectively. The dashed and solid curves are obtained by using the meshes of at least 15 and 20 division cells per wavelength in the frequency band of interest, respectively. They are found to be in excellent agreement with the measured data and the results obtained by the mode matching method [4]. This example verifies the capability of the present analysis in dealing with junctions of more general shapes.

V. Waveguide Transition with Transformer

It is much more difficult to design the transition between rectangular and dielectric-filled circular waveguides. The abrupt change in both the dielectric constant and the waveguide shape makes the analysis a great challenge. Fig. 6(a) shows a transition design between a standard WR-187 rectangular waveguide and a circular waveguide of diameter 0.44 in and filled with dielectric of $\epsilon_r = 16$. In the transition section, the circular dielectric rod intrudes into the rectangular waveguide region by a certain length l. FEM is very suitable for the analysis of such a transition structure.

The case of $l = 0$ denotes a step junction without transformer. As shown by the calculated results in Fig. 6(b), the transition is bad over the whole operating frequency band. An additional transformer section can greatly improve the transition property, as shown by the dashed curves in Fig. 6(b). By varying the section length, one may even achieve a matched design, say $l = 0.433$ in in this case, with zero reflection at a certain frequency. It is also possible to design a matched transition at other frequencies but choosing the diameter of the inserted rod d as another parameter. For example, Fig. 6(c) shows three designs of $(d, l) = (0.50$ in, 0.480 in), $(0.44$ in, 0.433 in), and $(0.38$ in, 0.384 in), which are matched at 5.17 GHz, 5.72 GHz, and 6.43 GHz, respectively. However, the bandwidth in which the return loss is less than -20 dB is in general small, about 5%, by such a single transformer design.

To achieve a wideband transition, it would be advantageous to consider the modified transformer design shown in Fig. 7. The inserted circular rod is made of an intermediate dielectric

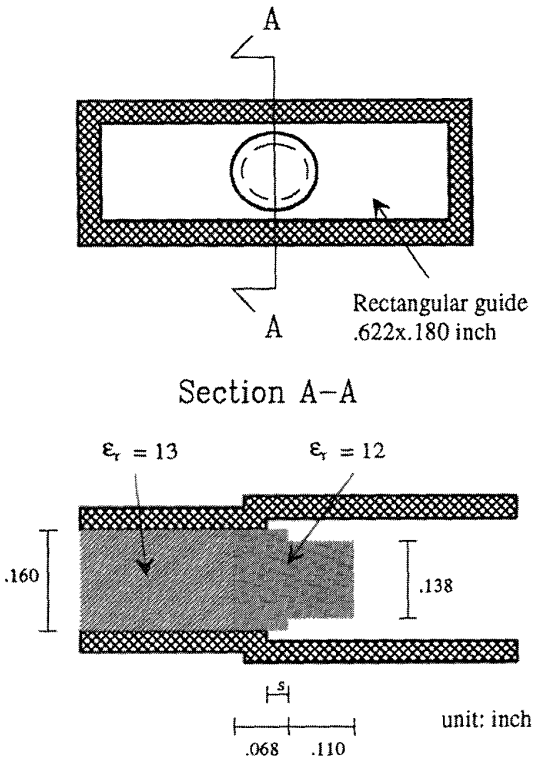

Fig. 7. A wideband transition design of modified transformer.

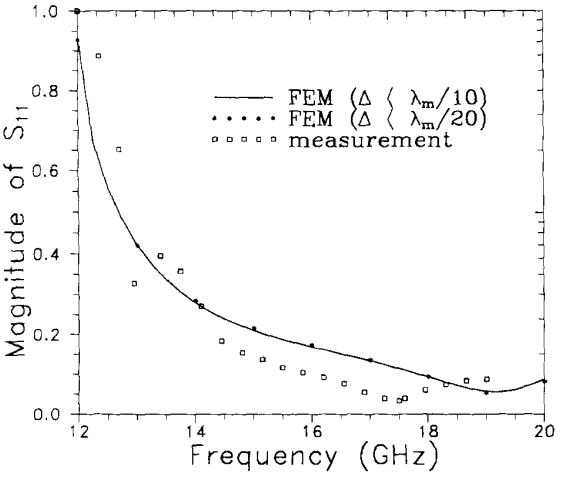

Fig. 8. Calculated and measured reflection coefficient for the transition structure in Fig. 7 in case of zero offset ($s = 0$).

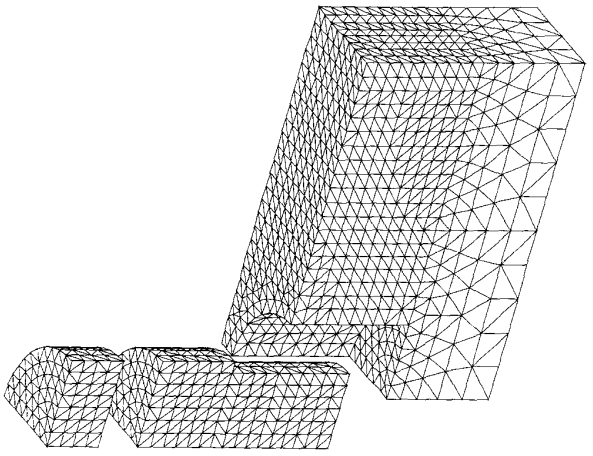

Fig. 9. Mesh for the transition structure shown in Fig. 7.

constant to provide additional impedance match. It has a step cut in the diameter and can be offset from the joint of the two metallic waveguides by a distance s.

The original design is performed for the case $s = 0$ in the industry by trial and error [20]. The solid curve in Fig. 8 shows the theoretical results obtained by using a mesh with at least ten cells per material wavelength. The convergency is assured by the comparison with the results obtained by employing a finer mesh of at least 15 cells per material wavelength.

Fig. 9 shows a 3-D plot of the finer mesh which consists of 17 301 tetrahedra. The three different material regions in the original structure are intentionally dissected to provide a closer look. Note the coarser mesh in the rectangular waveguide region, where the wavelength is about three times that in the material. The mesh includes 18 921 unknowns, although the matrix actually required in the program execution is symmetric and of a largest dimension of 739 only. The computation time for the scattering matrix per frequency is about 45 min by a notebook IBM/PC-486 with 8 mbyte RAM. It is interesting to compare the computation time of the present analysis with that of the commercial software HFSS [12]. The HFSS was employed for the analysis of a dual DR filter which is divided into 8073 tetrahedra [21]. It was reported that the computation time for each frequency is about 12 h on a HP-720/9000 workstation with 128 mbyte RAM.

The measured data [20] are also included in Fig. 8 for comparison. In light of the great challenge in fabrication control and measurement calibration for both the nonstandard waveguides, the measured data show reasonable agreement with the theoretical results. Both the theoretical and measured results confirm that this design, although more complicated in fabrication, can provide a larger bandwidth, about 15% in this case.

Furthermore, a design with even larger bandwidth can be accomplished by choosing a suitable offset s. Fig. 10 shows the magnitude of reflection coefficient with the offset as a parameter. With a small offset, it seems that there are two resonant frequencies: one nearly fixed at 13 GHz and the other inversely proportional to the length of the dielectric rod in the rectangular waveguide portion. Increasing the offset makes the two resonant mechanisms close to each other and consequently achieves a fruitful design at $s = 0.03$ in. The transition has a less than -20 dB return loss from 12.5 GHz to 18.5 GHz, which already covers the whole spectrum that the waveguides are designed for use. At a certain offset, say $s = 0.045$ in, the transition may even become a perfect match at 14.8 GHz. The return loss is smaller than -30 dB over a bandwidth of about 1.2 GHz.

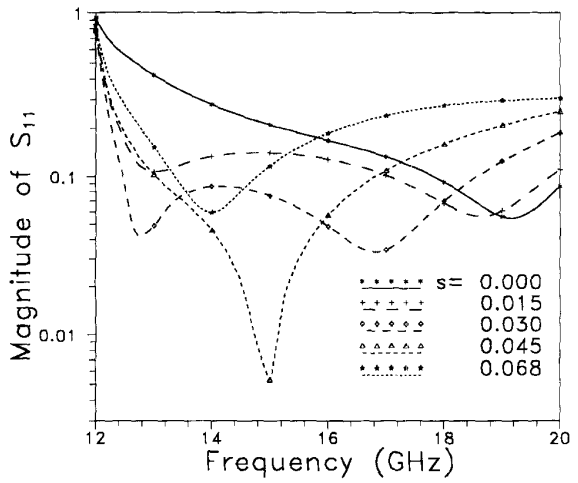

Fig. 10. Reflection coefficient for the transition structure shown in Fig. 7 with offset as a parameter.

VI. Conclusion

This paper employs a hybrid approach to deal with general 3-D waveguide junction problems, by combining the FEM for the irregular but finite-sized transition region and the mode expansion technique for the regular but semi-infinitely long waveguides. The approach is applied to design the transition between rectangular and dielectric-filled circular waveguides. Due to the change in both the dielectric constant and the waveguide shape, a simple design with abrupt step junction always results in intolerable return loss. Extending the dielectric into the rectangular waveguide portion significantly improves the transition performance. A perfect match design can even be achieved by choosing the dielectric rod of a suitable diameter and length. However, the bandwidth in which the return loss is less than -20 dB is in general small. A good transition of higher bandwidth can be accomplished by using material of intermediate dielectric constant. Based on this modified transformer, a nearly full band transition design has been demonstrated successfully. Even in some stringent systems which require a -30 dB return loss, successful transition design can be fulfilled by the modified transformer with a bandwidth of about 10%.

Acknowledgment

The author thanks T. Itoh of the University of California, Los Angeles, for the encouragement of this study.

References

[1] D. M. Pozar, *Microwave Engineering.* Reading, MA: Addison-Wesley, 1990, ch. 10.

[2] A. Wexler, "Solution of waveguide discontinuities by modal analysis," *IEEE Trans. Microwave Theory Tech.,* vol. MTT-15, pp. 508–517, Sept. 1967.

[3] Y. C. Shih, "The mode-matching method," in *Numerical Techniques for Microwave and Millimeter Wave Passive Devices,* T. Itoh, Ed. New York: Wiley, 1989, ch. 9.

[4] J. L. Fontecha and C. Cagigal, "Transition rectangular to circular waveguide by means of rectangular guides," *Int. J. Electromagnetic Computation, IEE,* pp. 378–381, 1991.

[5] E. A. Navarro, V. Such, B. Gimeno, and J. L. Cruz, "T-junctions in square coaxial waveguide; a FD-TD approach," *IEEE Trans. Microwave Theory Tech.,* vol. 42, pp. 347–350, Feb. 1994.

[6] S. K. Jeng and C. H. Chen, "On variational electromagnetics: Theory and application," *IEEE Trans. Antennas Propagat.,* vol. AP-32, pp. 902–907, Sept. 1984.

[7] R. B. Wu and C. H. Chen, "On the variational reaction theory for dielectric waveguides," *IEEE Trans. Microwave Theory Tech.,* vol. MTT-33, pp. 477–483, June 1985.

[8] Z. J. Cendes and J. F. Lee, "The transfinite element method for modeling MMIC devices," *IEEE Trans. Microwave Theory Tech.,* vol. 36, pp. 1639–1649, Dec. 1988.

[9] J. F. Lee, "Analysis of passive microwave devices by using three-dimensional tangential vector finite elements," *Int. J. Num. Modeling,* pp. 235–246, 1990.

[10] K. Ise, K. Inoue, and M. Koshiba, "Three-dimensional finite-element method with edge-elements for electromagnetic waveguide discontinuities," *IEEE Trans. Microwave Theory Tech.,* vol. MTT-39, pp. 1289–1295, Aug. 1991.

[11] A. Bossavit, "Solving Maxwell's equations in a closed cavity and the question of spurious modes," *IEEE Trans. Magn.,* vol. 25, pp. 702–705, Mar. 1990.

[12] Hewlet Packard, *Manual for High Frequency Structure Simulator HP85180A.*

[13] C. H. Chen and C. D. Lien, "The variational principle for nonself adjoint electromagnetic problems," *IEEE Trans. Microwave Theory Tech.,* vol. MTT-28, pp. 878–886, 1980.

[14] B. Delaunay, "Sur la sphére vide," *Bull. Acad. Science USSR VII: Class. Sci. Mat. Nat.,* pp. 793–800, 1934.

[15] Z. J. Cendes, D. Shenton, and H. Shahnasser, "Magnetic field computation using Delaunay triangulation and complementary finite element methods," *IEEE Trans. Magn.,* vol. MAG-19, pp. 2551–2554, Nov. 1983.

[16] D. F. Watson, "Computing the n-dimensional Delaunay tessellation with applications to Voronoi polytopes," *Computer,* pp. 48–57, 1977.

[17] J. C. Cavendish, D. A. Field, and W. H. Frey, "An approach to automatic three-dimensional finite element mesh generation," *Int. J. Numer. Methods Eng.,* vol. 21, pp. 329–347, 1985.

[18] K. Forsman and L. Kettunen, "Tetrahedral mesh generation in convex primitives by maximizing solid angles," *IEEE Trans. Magn.,* pp. 3535–3538, 1994.

[19] E. Hinton and D. R. J. Owen, *Finite Element Programming.* New York: Academic, 1977.

[20] D. C. Niu, "Analysis of complex waveguide structures using the finite-difference time-domain method," masters thesis, University of California, Los Angeles, 1994. The structure is proposed and measured by the Microwave Application Group, Santa Maria, CA.

[21] H.-R. Chuang, J.-W. Huang, C.-C. Wei, and J. L. C. Chang, "3D FEM simulation and experimental measurements of microwave microstrip dielectric-resonator filters," *Microwave Opt. Technol. Lett.,* vol. 8, pp. 196–200, Mar. 1995.

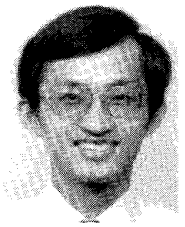

Ruey-Beei Wu was born in Tainan, Taiwan, Republic of China, in 1957. He received the B.S.E.E. and Ph.D. degrees from National Taiwan University, Taipei, Taiwan, in 1979 and 1985, respectively.

In 1982, he joined the faculty of the Department of Electrical Engineering, National Taiwan University, where he is now a Professor. He was a Visiting Scholar at the IBM East Fishkill Facility, New York, from March 1986 to February 1987, and in the Electrical Engineering Department, University of California, Los Angeles, from August 1994 to July 1995. His areas of interest include computational electromagnetics, dielectric waveguides, edge slot antennas, wave scattering of composite materials, transmission line and waveguide discontinuities, and interconnection modeling for computer packaging.